Surfaces and Interfaces 76 (2025) 107906

Contents lists available at ScienceDirect

Surfaces and Interfaces

journal homepage: www.sciencedirect.com/journal/surfaces-and-interfaces

Simple and fast wettability control of aminosilanized surfaces with carboxylic acids

Andraž Černoga [a], Jelena Papan Djaniš [a,c], Darja Lisjak [b], Jernej Iskra [a], Griša Prinčič [a,*]

[a] Faculty of Chemistry and Chemical Technology, University of Ljubljana, 1000 Ljubljana, Slovenia
[b] Department for the Synthesis of Materials, Jožef Stefan Institute, 1000 Ljubljana, Slovenia
[c] Centre of Excellence for Photoconversion, Vinča Institute of Nuclear Sciences, National Institute of the Republic of Serbia, University of Belgrade, 11351 Belgrade, Serbia

ARTICLE INFO

Keywords:
Organic coatings
Hydrophobicity
Wettability
APTMS
Carboxylic acids
Silanization

ABSTRACT

This study investigates the rapid and reversible transition between hydrophilic and hydrophobic states on aminosilanized glass substrates using ion pair formation between surface-bound amines and organic/inorganic acids. Glass surfaces were prepared via piranha solution treatment, followed by drying and chemical vapor deposition of 3-aminopropyltrimethoxysilane. Water contact angle measurements revealed a sharp transition in surface wettability upon treatment with mineral acids while treatment with carboxylic acids shows a strong dependence on carbon chain length. This approach utilizes non-fluorinated long-chain carboxylic acids as environmentally friendly alternatives to PFAS, aligning with current global efforts for sustainable engineering. The system's ability to cycle between hydrophilic and hydrophobic states within min per cycle demonstrates the efficiency of this ion pair-driven approach compared to conventional methods. Work offers insights into optimizing surface modifications for applications such as self-cleaning, anti-icing, microfluidics and dynamic wettability control without the need for prolonged processing times and complicated and expensive equipment.

1. Introduction

In nature, there are many organisms who have evolved unique solutions to adapt to the environment, providing inspiration to design advanced materials. The special surface wettability formed by a combination of hierarchical structures and chemical compositions contributes to some unique and special functions. Among them, many biological surfaces show superhydrophobicity, for example, micropapillae and nanostructures on the lotus leaf surface are associated with a waxy material for achieving superhydrophobic and self-cleaning properties [1,2]. Nowadays, in the modern world, functional surfaces with reversible hydrophilic-hydrophobic transitions are widely used for self-cleaning [3,4], fog collection [5], anti-icing [6], droplet transportation [7–11], and recently, as anti-counterfeiting technology [12]. Inspired by nature, it is possible to induce the hydrophobic-hydrophilic (Cassie-Baxter-Wenzel) transition using different external stimuli such as light [13,14], temperature [15,16], pH [17,18], ion exchange [19], voltage [15,20], magnetic field [21] or, recently, electron beams [22]. The adsorption/removal or phase change of hydrophilic or hydrophobic functional groups on the surface is a key factor in the reversible transformation of surface wettability. Jiang et al. prepared a micro-patterned substrate and deposited a monolayer of CF_3-azobenzenes that change wettability with UV light [23]. Diarylethenes were also found to be another excellent choice for light-sensitive switchable wettability [24] as well as oxidation of TiO_2 nanoparticles on the surface [7]. Thermal oxidation, ultraviolet (UV) irradiation combined with thermal oxidation, and UV irradiation combined with chemical modification are the primary techniques to induce change in wettability. Thermal oxidation at 150 °C for 4 h accelerates the adsorption of airborne organic molecules, leading to an increase of C—C/C—H groups and a contact angle of 160° on the textured brass surface [25]. Although it achieves the cyclic transition between superhydrophobicity to superhydrophilicity, a long processing time and metal oxides are the disadvantages of this method. The method of UV irradiation is to use UV light to remove or oxidize adsorbed hydrophobic groups (C—C/C—H) into hydrophilic groups (C—O, —OH), thereby reducing the contact angle. However, the UV irradiation process requires at least 9 h [25]. Despite many developed methods, most of them still require several hours, and expensive and complicated equipment to achieve the desired switch from hydrophilic to hydrophobic surface state or *vice versa*, respectively. Not only that, traditional methods for creating hydrophobic surfaces often rely on fluorinated compounds (PFAS), which are increasingly being phased out

* Corresponding author.
E-mail address: grisa.grigorijprincic@fkkt.uni-lj.si (G. Prinčič).

https://doi.org/10.1016/j.surfin.2025.107906
Received 12 February 2025; Received in revised form 25 September 2025; Accepted 16 October 2025
Available online 16 October 2025

due to their environmental persistence and health risks. In response to these concerns, there is a growing interest in developing PFAS-free surface modification strategies [35].

To address these considerations, the present study involved optimization of glass substrate (amino)silanization and determination of reversible hydrophilic/hydrophobic behavior of such coatings, based on the adsorption and desorption (ion pair formation) of organic and inorganic acids with varying hydrophilic characters. We systematically studied the initial preparation parameters of the glass surface like piranha treatment, drying protocols and the chemical vapor deposition conditions of 3-aminopropylsilane. Aminosilanized samples were then used to investigate their reversible and switchable wettability properties, achievable within minutes per cycle using simple acid/base treatments. Importantly, this approach avoids fluorinated compounds and requires no specialized equipment, offering a practical and environmentally conscious alternative to light, heat, or voltage-based methods. The study further reveals how acid chain length and surface protonation influence wettability dynamics, providing new mechanistic insights into the role of ion-pair stability in dynamic surface modification. Such surfaces hold potential for diverse applications, including self-cleaning, anti-icing, microfluidics, and responsive interfaces and thereby advancing the field of surface and interface science through both conceptual simplicity and performance robustness.

2. Experimental section

2.1. Glass substrate preparation

Incisions approximately 15 mm apart were made in the glass slides (Assistent, 76 mm × 26 mm) using a hardened steel blade. The slides were then broken by hand into pieces approximately 15 mm × 26 mm. The cut slides were washed in an Erlenmeyer flask with acetone (Honeywell) and sonicated in the solvent using ultrasound (Elma, X-tra 30 H). Each slide was individually rinsed with deionized water and placed against the wall of a beaker. The prepared piranha solution (conc. H_2SO_4:H_2O_2 3:1) was poured into the beaker, ensuring all slides were covered, and the beaker was covered with a watch glass. The duration of immersion in the piranha solution was varied. After hydroxylation in the piranha solution, all slides were rinsed simultaneously in an Erlenmeyer flask under running deionized water for approximately 5 min and then rinsed with MeOH (J.T. Baker). The slides were dried on a Teflon rack in an oven (Kambič SP-55) at 150 °C. The drying time was varied.

2.2. Chemical vapor deposition of aminosilanes

After drying, Teflon lined steel reactors (see Fig. 3A) were purged with Ar, an HPLC vial was placed in the center of the reactor, and three glass slides were arranged around it and 50 μL of 3-aminpropyltrimethoxy silane (APTMS) was added to the vial with a pipette. The reactors were purged with Ar once more, sealed, and placed in an oven heated to a specified temperature (ranging from 80 °C to 150 °C) for 24 h. The following day, the reactors were opened in a fume hood. The glass slides were transferred into a solution of *N,N*-diisopropylethylamine (DIPEA) (1 mL/100 mL in MeCN). After 5 min, a slide was removed from the solution and rinsed first with MeCN and then with deionized water. Such substrates were used for further experimentation. Note: in several experiments where reactor liners were used multiple times, the glass slides exhibited a milky white, opaque coating. This due to Teflon liner degradation (see Supporting Information for more details).

2.3. Surface amine density determination

Fresh aminosilanized glass substrates were placed into an aqueous solution of trinitrophenol (TNP) (17 mg/L). After 6 min in the TNP solution, the slides were removed, and excess solution was rinsed off with deionized water. Slides turned yellow (see Figure S-1 and Figure S-3). Slides were then immersed into K_2CO_3 solution (20 g/L, 4 mL) until all the yellow coloration from the surface was washed into the solution (approx. 1 min). Concentration of TNP in the solution was determined with spectral absorbance measurement at $\lambda = 368$ nm. The surface amine density was determined according to:

$$\textit{number of } NH_2 \textit{ groups on surface } (\gamma) = \frac{N_A \times C_{TNP} \times V_{K2CO3}}{M_{TNP} \times S \times 1000} \left[\frac{\text{amine}}{\text{cm}^2}\right] \quad (1)$$

$C_{(TNP)}$ was determined according to equation from linear curve ($Y = 53.54X + 0.0016$) (see Figure S-2). N_A is Avogadro constant, V_{K2CO3} is the volume of potassium carbonate solution in mL, M_{TNP} is the molar mass of TNP and S is the surface area of glass slides in cm^2.

Streaming potential (Zeta potential) of glass slides was measured using a SurPASS electrokinetic analyzer (Anton Paar GmbH, Graz, Austria) at 19–22 °C in 1 mmol/L potassium bromide.

2.4. Contact angle determination

To evaluate the wettability of the specimen surfaces, we tested the water contact of the specimens using a contact-angle measuring instrument. Measurements were performed using an Attension Theta Light optical tensiometer and *One Attension* software. The slide was placed on the tensiometer platform, the camera focus was adjusted, a 3 μL water droplet was deposited on the slide, and the static contact angle θ [°] of the droplet with the glass surface was recorded. Each measurement was repeated twice.

2.5. Hydrophilic/Hydrophobic cycling of amine-coated glass substrates

The glass slides were immersed in the solution of the appropriate carboxylic acid in MeCN/H_2O 1:1 for 2 min, rinsed with water, and dried with compressed air. After the measurement of contact angle, the slide was immersed in a solution of K_2CO_3 (20 g/L), rinsed with deionized water, and then immersed in the next acid solution. The previously described procedure was repeated.

3. Results and discussion

3.1. Substrate preparation and optimization of glass silanization with chemical vapour deposition (CVD) process

We were following the stepwise protocol depicted in Fig. 1. Hydroxylation of glass surfaces before silanization is a critical step in modifying the surface chemistry and enhancing the effectiveness of subsequent silanization processes. Surface hydroxylation of substrates increases the number of available reactive hydroxyl (−OH) groups on the surface and enables a larger number of silane molecules to react on its surface. Usually, this is accomplished by treatment of substrates with plasma [26] or immersion into an oxidizing medium like piranha solution for a certain amount of time [27–29].

We were interested in the time parameter of this treatment. To assess the surface hydroxylation level the wettability was evaluated by the water contact angle measurement of the as-prepared samples prior and after piranha treatment. We can observe a very sharp drop in hydrophobicity of the glass surface when it was exposed to hot piranha solution (Fig. 2A). Surface reaches a contact angle of $<10°$ (superhydrophilic character) after only a few seconds in the acid/peroxide mixture. Most of siloxane groups on the surface of glass have been converted to silanol groups and the hydrophilicity of the surface no longer changes. Longer times apparently do not aid to an increased number of reactive hydroxyl groups on the surface.

Due to its strongly hydrophilic nature, molecules of water are bound in several layers on the surface of hydroxylated glass. Only at elevated temperatures this layer of water can be evaporated, leaving behind just

Fig. 1. Stepwise protocol for aminosilanization of glass substrates with CVD method.

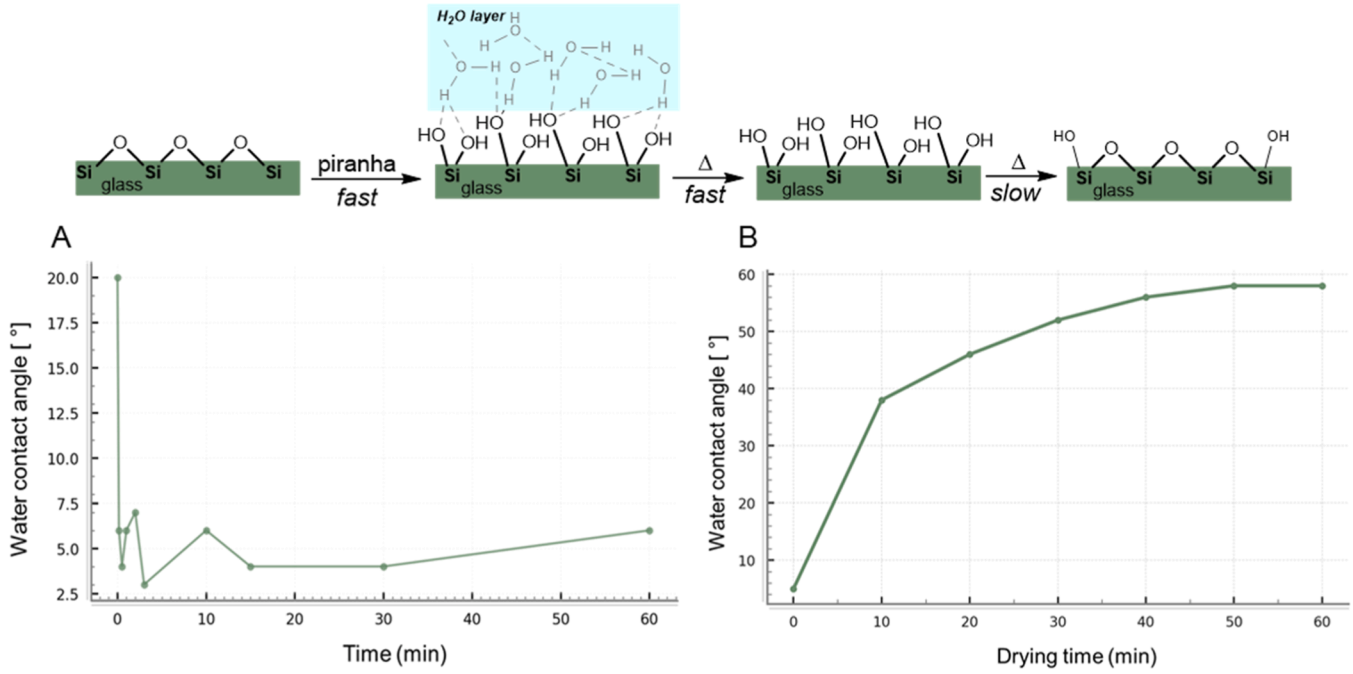

Fig. 2. (A) Water contact angle of glass surfaces after varying times in piranha solution. (B) Water contact angle of glass surfaces after varying drying times (after hydroxylation in piranha solution for 5 min).

the hydroxylated surface [30]. However, at elevated temperatures of > 150 °C, the surface silanol groups start to convert back to siloxane groups hampering the surface's functionalization. Since D'Souza at al. have shown that at 150 °C mostly water is evaporated from the surface and the reversion of silanol groups to siloxane is slow [31] (Fig. 2B), we opted for the examination of drying times at this temperature.

In contrast to hydroxylation of the glass surface with piranha solution the reversible reaction at 150 °C is much slower. In the first 10 min of heating the contact angle sharply increases back to 35° indicating a decrease in hydrophilicity. We can attribute this fast-initial change to the evaporation of surface bound water from glass surface. After the thickness of water layer has reached its equilibrium at that temperature the much slower and steady decrease in the hydrophilicity of samples can be attributed to the formation of siloxane groups from silanol groups (Fig. 2).

While the duration of hydroxylation in the piranha solution is not crucial, we were more interested in how the drying time affects silanization and consequently the hydrophobicity of glass. Silanization was carried out in Teflon reactors, into which we placed 50 μL of APTMS along with the hydroxylated glass slides dried for the selected durations. The reactor was purged with argon, sealed, and placed in an oven at 150 °C for 24 h (Fig. 3A). The number of amino groups attached to the glass was determined spectroscopically using the TNP binding method (Fig. 3B) [32]. Number of amine groups on the surface of our slides prepared with chemical vapor deposition (CVD) method was compared with commercially available substrates like NANOCS GS-AM-25 glass slides. Interestingly, the TNP determination method did not detect any amine groups on the commercially available NANOCS GS-AM-25 glass slides, indicating the absence of reactive amines or an insufficient amine density on their surface. An increasing trend in the number of amine groups per unit area can be observed with longer drying times before silanization, up to a peak at 15 min, followed by its decrease (Fig. 3C). This behavior is attributed to the evaporation and thinning of the water layer on the glass surface, which initially exposes more reactive silanol groups, allowing greater reaction with aminosilane molecules. Beyond 15 min, the formation of siloxan groups from silanol prevails and the efficiency of silanization decreases.

Modification of the glass surface was also monitored by measuring the streaming potential potentials of glass slides (Fig. 4). Nontreated glass has a slightly negative surface, while after piranha treatment the glass surface possesses more negatively charged –OH groups and zeta potential decreases. After aminosilanization, the zeta potential is shifted to a highly positive value due to positively charged amino groups bonded at the glass surface.

We also investigated the effect of silanization temperature on the number of accessible amino groups. We used glass slides that were previously hydroxylated in a piranha solution for 5 min and then dried in an oven at 150 °C for 15 min. Silanization was performed following the same procedure as in the previous experiment, with the difference being the temperature at which the silanization reaction took place. An interesting trend can be observed here, where the number of amino groups first decreases with an increasing temperature, and then sharply jumps at the temperature of 150 °C (Fig. 3D). The polymerization of (3-aminopropyl)trimethoxysilane (APTMS) and its reaction with -OH groups on substrate surfaces is a highly complex process influenced by various parameters, including temperature, water content (both in liquid and gas phases), and pH. Aminosilanes can adopt multiple conformations on the surface, forming layers of varying structural organization. However, not all conformations are suitable for applications requiring exposed amine groups for subsequent reactions. Typically,

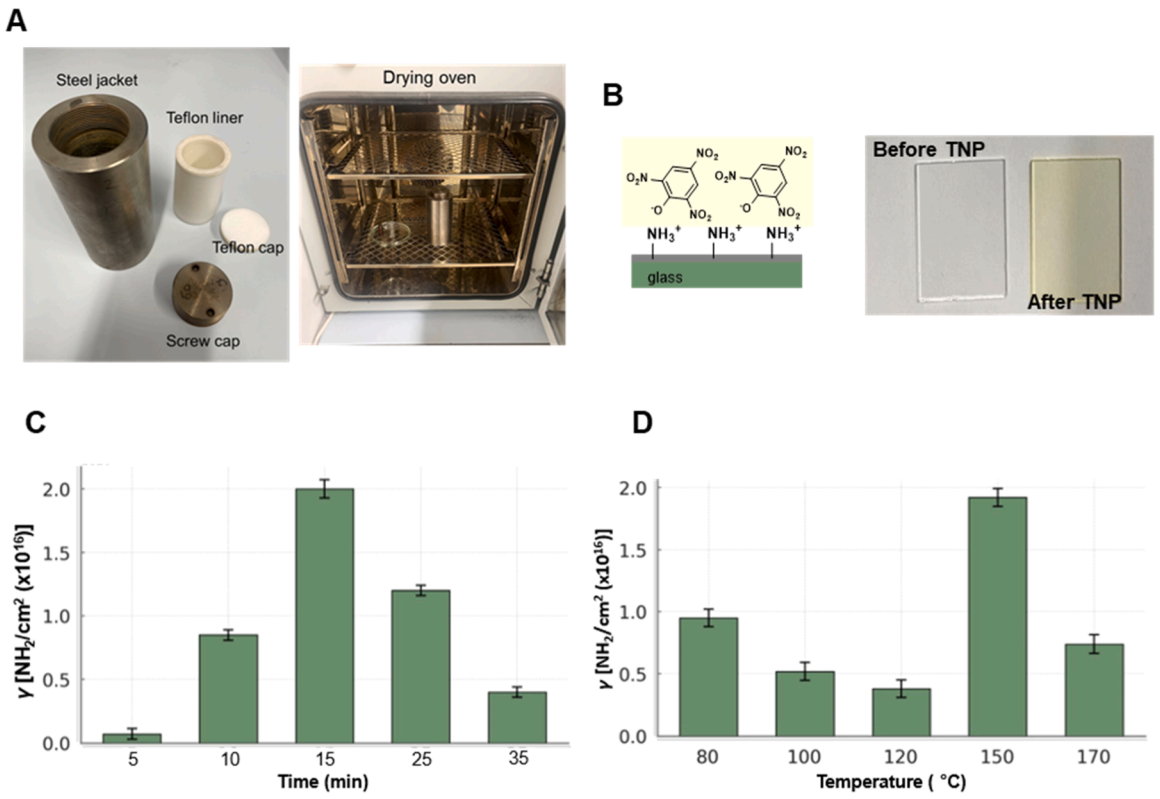

Fig. 3. (A) Teflon lined steel reactor used for CVD, PT100 thermocouple controlled ventilation oven with a steal reactor. (B) TNP binding to surface of aminosilanized glass. Glass slides before and after immersion into TNP solution. Yellow colouring is visible on the surface due to TNP binding to the amines. (C) Effect of drying time on the number of accessible amine groups on glass surface at 150 °C. (D) Effect of CVD reaction temperature on the number of accessible amine groups on the glass surface (drying time 15 min at 150 °C). * Error bars represent ±1 SD.

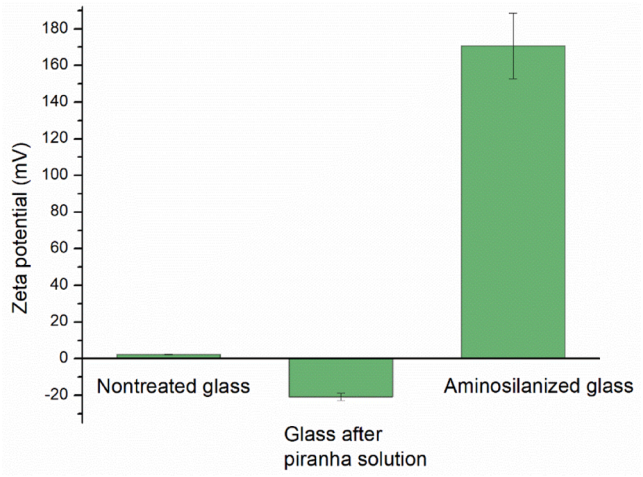

Fig. 4. Streaming potential at pH 3.5 of nontreated glass, glass after treatment with piranha solution, and CVD aminosilanized glass. * Error bars represent ±1 SD.

higher reaction temperatures result in denser packing of aminopropyl chains and increased covalent bond formation between APTMS molecules, which can significantly impact surface functionality [33,34].

3.2. Reversible hydrophobicity effect of different acids on glass surface

With optimal aminosilanization conditions in hand, we continued our research on the effect of binding of acids to aminosilanized glass and the resulting changes in hydrophobic properties. The aminated glass slides prepared at optimal conditions were immersed for 2 min in a solution of the selected acid (mineral or carboxylic; HCl, H_2SO_4, acetic acid and citric acid) in a 1:1 MeCN/water mixture to protonate the amine groups on the surface and form a monolayer of A^- ●●●●$^+NH_3$ salts (Fig. 5). The excess acid was rinsed off with water, dried with compressed air, and the contact angle was measured.

We first tested the effect of protonation of amino-functionalized glass surface with classical inorganic acids. The contact angle of amino-functionalized glass was 34° (Fig. 6). Upon treatment with acids the surface becomes much more hydrophilic when amine groups are protonated. Contact angles as low as 19° were achieved with acetic acid. The behavior of small and polar organic acids (acetic and citric) is as expected, showing similar low contact angles to mineral acids, consistent with the polarity of acetic and citric acids.

To investigate further, we wanted to understand how organic acids with longer carbon chains (C_7 – C_{20}) would influence surface hydrophobicity. Perfluorooctanoic acid (PFOA) was used as a standard since perfluorinated compunds were classicaly used for preparation of hydrophobic surfaces. Since per- and polyfluoroalkyl substances (PFAS) molecules, such as PFOA, are increasingly recognized for their environmental persistence and adverse health effects, they are being progressively phased out and banned from consumer products [35]. In light of this, we focused on exploring alternative carboxylic acids with long carbon chains as substitutes for PFOA. Our study included carboxylic acids with a varying number of carbon atoms, ranging from C_2 (acetic acid) to C_{20} (eicosanoic acid), to evaluate how the chain length influences the surface hydrophobicity (Fig. 7B). From Fig. 7B we can observe a trend of increasing contact angles with number of C atoms in carboxylic acid bound to the surface. Carboxylic acids with 2, 7, 10, 18 and 20 carbon atoms have contact angles of 16°, 54°, 70° 98° and 103°, respectively, demonstrating the positive effect of chain length on hydrophobicity. To our surprise, simple and environmentally benign

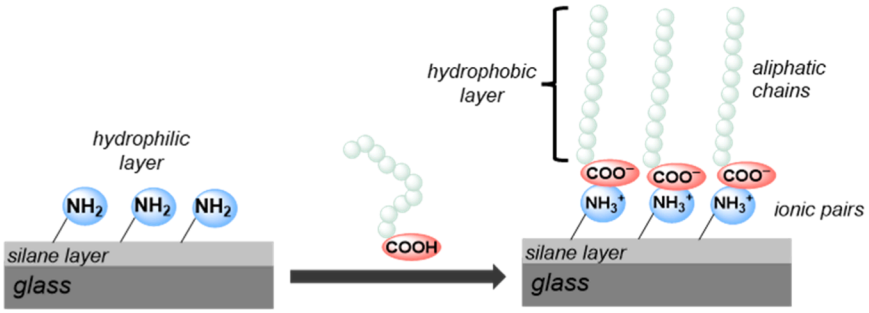

Fig. 5. Ionic pairs formation on the surface of aminosilanized glass substrate with long chain carboxylic acids. The formation of ionic pairs prevents the acids from being washed off the surface. Long hydrophobic chains form a hydrophobic monolayer on the surface.

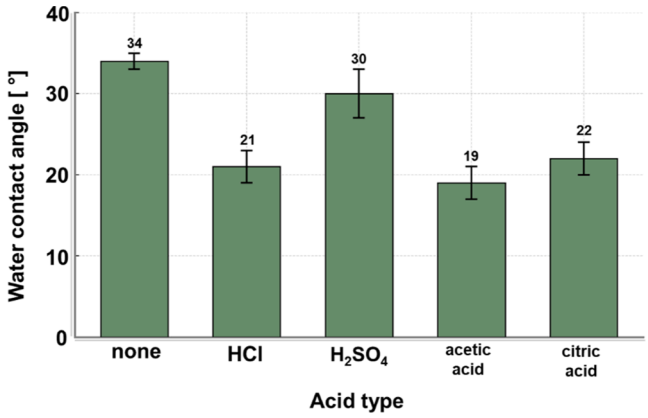

Fig. 6. Water contact angles of aminosilanized glass substrates after amine groups on the surface were protonated with different mineral and organic acids. * Error bars represent ±1 SD.

stearic and eicosanoic acid performed even better than PFOA. We also demonstrate that a selective portion of the aminosilanized glass surface can be tailored to become either hydrophilic or hydrophobic. This is achieved simply by exposing it to different types of acids (Fig. 7C and Figure S-5). Besides for water, contact angles for oil (olive oil) and heptane were also determined as representatives of semi polar and nonpolar liquids. Oil behaves very similar to water with highest contact angle measured when aminosilanized glass was coated with PFOA. Heptane contact angles were intrinsically low due to very low surface tension of the liquid.

3.3. Reversible hydrophilic/hydrophobic coating

We further demonstrated the reversibility of interactions with the acids that yielded the highest contact angle (perfluorooctanoic acid, PFOA) and the lowest contact angle (hydrochloric acid) in the previous experiment. To assess the durability and consistency of the hydrophobic and hydrophilic states, the aminosilanized glass slides were subjected to multiple cycles of acid exposure and rinsing. Each glass slide was immersed for 2 min in a 1:1 water:acetonitrile solution containing the selected acid (sulphuric acid or PFOA) to protonate the amine groups on the surface, thereby modulating the surface hydrophobicity. After each immersion, the slides were thoroughly rinsed with water to remove any excess acid, dried with compressed air, and the contact angle was measured to evaluate the surface's hydrophobic or hydrophilic state. This process was repeated for a total of 30 cycles on the same glass slide sample, resulting in 60 acid changes per sample (Fig. 7A).

From Fig. 7A, we can observe a consistent trend in the contact angles for each acid throughout the cycles, indicating the reproducibility and stability of the surface modifications. The contact angles for PFOA remained consistently high, reinforcing its hydrophobic effect, while sulphuric acid maintained low contact angles, confirming its hydrophilic influence. Notably, after 30 cycles, there was no significant loss in the reliability of the hydrophobic/hydrophilic switching mechanism of the glass surface, demonstrating that the system is robust and capable of repeated reversible modifications without degradation of performance. This consistency suggests that the acid treatments can be reliably used for dynamic surface modifications in applications requiring adjustable wettability.

3.4. Possible explanation of reversible hydrophilicity-hydrophobicity mechanism

The effect of chain length on increasing hydrophobicity of surface starts to diminish after C_{18} atoms (Fig. 7B). We can attribute this to structural differences affecting molecular packing on the glass surface [36,37]. While moderate chain lengths (C_{16}–C_{18}) promote dense and ordered monolayer formation through van der Waals interactions between aligned hydrocarbon chains, longer chains (C_{20}) introduce greater flexibility and conformational disorder. As chain length increases, entropic factors promote tilting, folding, or less ordered packing of the chains relative to the surface normal, which reduces the effective surface hydrophobicity despite the longer hydrocarbon backbone. Similar effects have been observed in self-assembled monolayers where excessive chain length leads to imperfect organization and loss of surface performance [38] (Fig. 8). These findings suggest that while longer carbon chains can enhance hydrophobicity, there are practical limits due to molecular packing and interaction distances that should be considered when designing surfaces for optimal wettability control.

To support the proposed ion pair formation between surface amines and adsorbed acids we conducted X ray photoelectron spectroscopy (XPS) analysis of the functionalized glass surfaces conjugated with acids. In the N 1s region, aminosilanized glass exhibited a NH_3^+:NH_2 ratio of 16.1:83.9. After treatment with acids this shifted to 20.2:79.8 for Arachidonic acid and 27.0:73.0 for PFOA (Figure S-6). C 1s spectra shows an increase in the O—C═O component at 288.8 eV, rising from 1.92 % in aminosilanized glass to 2.07 % with arachidonic acid and 2.92 % with PFOA (Figure S-7). These changes are consistent with acid–amine ion pair formation on the surface (Tables S1 and S2). F 1s spectra show a broad CF_2 peak from PFOA (Figure S-8). Full spectral data and peak assignments are provided in the Supporting Information.

3.5. Possible application of aminosilanized surfaces with reversible hydrophilic-hydrophobic character

To date, numerous applications utilize surface chemistry responsiveness. For instance, surfaces can exhibit reversible hydrophilic-hydrophobic behaviour in response to changes in pH, temperature, gas exposure, or ion concentration, offering significant potential in fields such as wastewater treatment, oil-water separation, microfluidics, biosensors, sensor detection, droplet storage, and germicidal applications [39]. Glass surfaces with switchable hydrophilic-hydrophobic

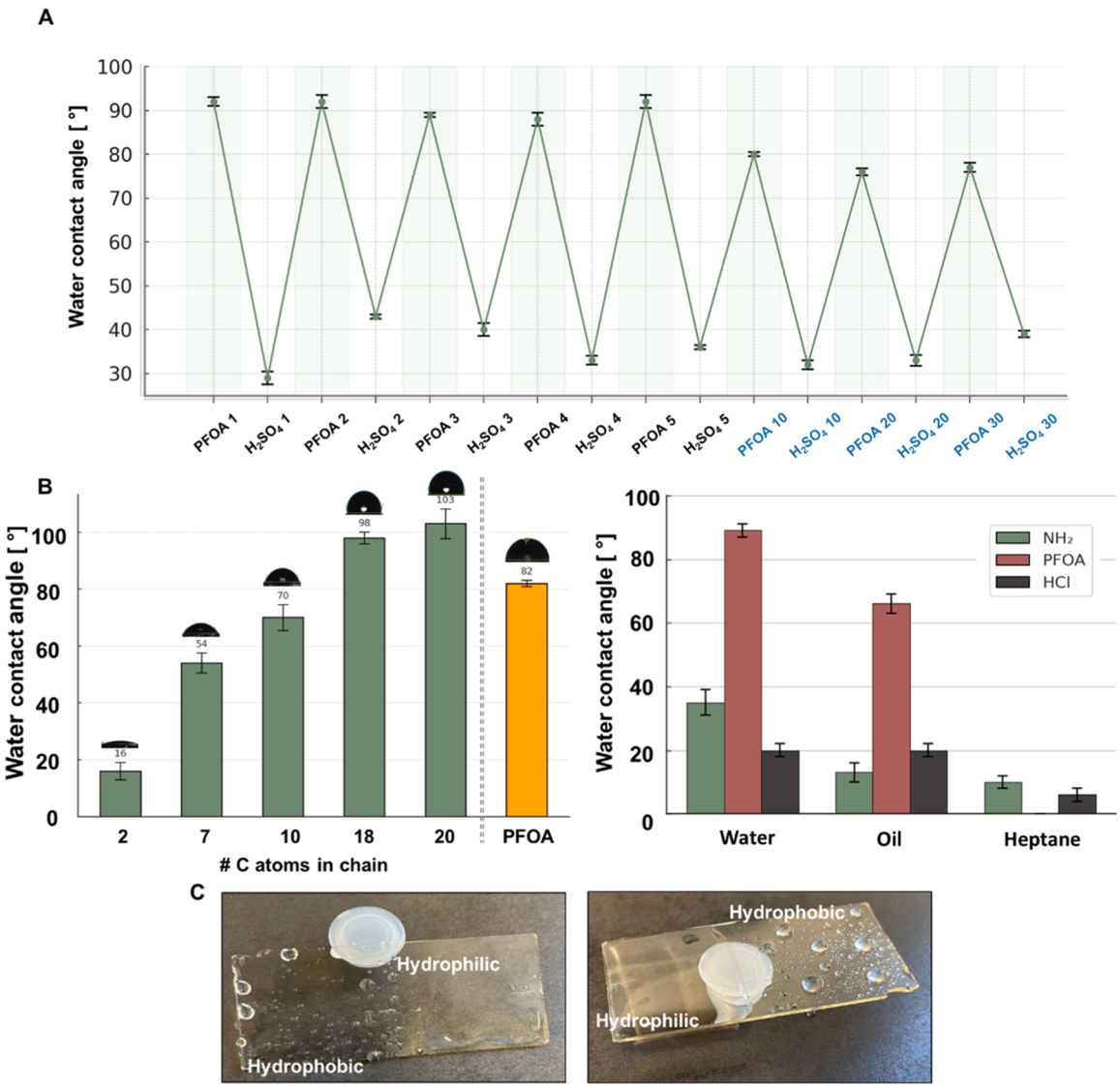

Fig. 7. (A) Cycling of hydrophobic to hydrophilic character of aminosilanized glass substrates with either PFOA or H_2SO_4. 30 cycles were performed without the loss of fidelity. (B) Left: Water contact angle determination for aminosilanized glass substrates protonated with carboxylic acids with varying chain lengths from C_2 (acetic acid) to C_{20} (eicosanoic acid) atoms in their chains. The longer the chain, the more hydrophobic character of the surface. Note that PFOA performs substantially worse than nonfluorinated carboxylic acids (C_{18} and C_{20}). Right: Contact angle comparison for Water, oil and heptane on glass slides functionalized with only amines, PFOA and HCl. (C) Examples of two glass slides with varying hydrophobic-hydrophilic surface. Half of the slide was made hydrophobic with C_{20} carboxylic acid and the other half was made hydrophilic with sulfuric acid. Slides were then dipped into water to display the difference in surface character. * Error bars represent ±1 SD.

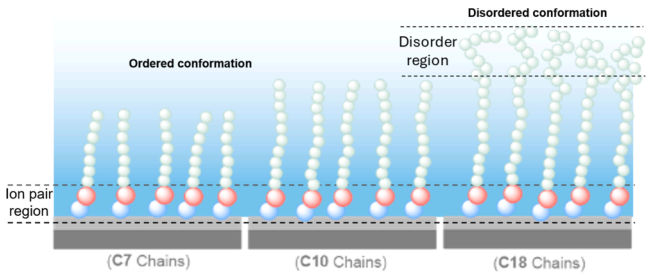

Fig. 8. Effect of chain length, molecular packing and electric field strength from ion pairs on the surface. The strength of electric field drops as distance from the ion pairs increases.

properties may also find use in smart homes, providing dirt protection and self-cleaning capabilities (Fig. 9) [40]. Recent work has also demonstrated the integration of reversible wettability into 3D-printed surfaces, expanding potential applications in advanced manufacturing and smart material design [41].

4. Conclusions

This study demonstrates a rapid and reversible method for controlling surface wettability on aminosilanized glass substrates through ion pair formation between surface-bound amines and acids. By optimizing the silanization process and utilizing organic and inorganic acids, we achieved fast wettability transitions within min, offering a significant improvement over conventional methods that require longer processing times and complex equipment. The temperature of silanization, particularly near the boiling point of (3-aminopropyl)trimethoxysilane, proved critical in maximizing surface amine density. We also found that the hydrophobicity of the surface increases with the length of the carboxylic acid's carbon chain, demonstrating the ability of the system to modulate the hydrophobicity of the surface. The system exhibited stable and repeatable wettability switching over multiple cycles, making it a

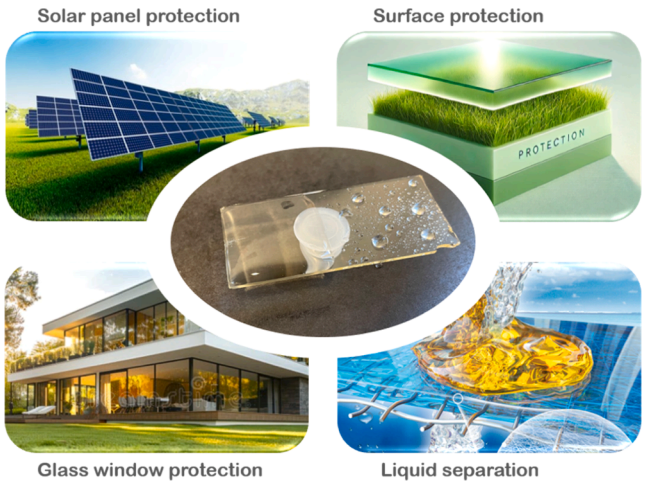

Fig. 9. Potential applications for glass with reversible hydrophobic-hydrophilic character. Examples are: Self-cleaning surface of solar panels, protection of surfaces like panels for houses and roofs, self-cleaning window for homes and liquid separation techniques.

promising approach for applications requiring dynamic surface properties, such as self-cleaning and anti-icing technologies. In contrast to conventional stimuli-responsive methods (light, temperature, electric field), our system achieves reversible wettability control rapidly, without requiring external devices or extended processing times. Additionally, long term stability, abrasion resistance and chemical durability of coatings were not evaluated. These constraints highlight that the findings represent a proof-of-concept framework rather than a fully validated application-ready system.

CRediT authorship contribution statement

Andraž Černoga: Data curation, Conceptualization. **Jelena Papan Djaniš:** Methodology, Formal analysis, Data curation, Conceptualization. **Darja Lisjak:** Funding acquisition, Formal analysis, Data curation. **Jernej Iskra:** Project administration, Funding acquisition, Formal analysis. **Griša Prinčič:** Writing – review & editing, Writing – original draft, Visualization, Validation, Supervision, Methodology, Investigation, Formal analysis, Data curation, Conceptualization.

Declaration of competing interest

The authors declare that they have no known competing financial interests or personal relationships that could have appeared to influence the work reported in this paper.

Acknowledgements

The authors acknowledge the financial support of the Slovenian Research and Innovation agency through the research core funding (Grant No. P1-0418, P1-0134, P2-0089 and J2-2495), and the CEMM Nanocenter for a SurPASS electro kinetic analyzer. We would also like to thank dr. Boštjan Genorio for XPS analysis and interpretation.

Supplementary materials

Supplementary material associated with this article can be found, in the online version, at doi:10.1016/j.surfin.2025.107906.

Data availability

Data will be made available on request.

References

[1] H. Li, Y. Duan, Y. Shao, Z. Zhang, L. Ren, Advances in organic adsorption on hydrophilic hierarchical structures for bionic superhydrophobicity: from fundamentals to applications, J. Mater. Chem. A 12 (2024) 14885–14939, https://doi.org/10.1039/D4TA00456F.
[2] L. Feng, S. Li, Y. Li, H. Li, L. Zhang, J. Zhai, Y. Song, B. Liu, L. Jiang, D. Zhu, Superhydrophobic surfaces: from natural to artificial, Adv. Mater. 14 (2002) 1857–1860, https://doi.org/10.1002/adma.200290020.
[3] J. Zheng, S. Bao, P. Jin, TiO2(R)/VO2(M)/TiO2(A) multilayer film as smart window: combination of energy-saving, antifogging and self-cleaning functions, Nano Energy 11 (2015) 136–145, https://doi.org/10.1016/j.nanoen.2014.09.023.
[4] S.G. Lee, D.Y. Lee, H.S. Lim, D.H. Lee, S. Lee, K. Cho, Switchable transparency and wetting of elastomeric smart windows, Adv. Mater. 22 (2010) 5013–5017, https://doi.org/10.1002/adma.201002320.
[5] Y. Peng, Y. He, S. Yang, S. Ben, M. Cao, K. Li, K. Liu, L. Jiang, Magnetically induced fog harvesting via flexible conical arrays, Adv. Funct. Mater. 25 (2015) 5967–5971, https://doi.org/10.1002/adfm.201502745.
[6] P. Irajizad, M. Hasnain, N. Farokhnia, S.M. Sajadi, H. Ghasemi, Magnetic slippery extreme icephobic surfaces, Nat. Commun. 7 (2016) 13395, https://doi.org/10.1038/ncomms13395.
[7] X. Liu, Y. Wei, F. Tao, X. Zhang, L. Gai, L. Liu, All-water-based superhydrophobic coating with reversible wettability for oil-water separation and wastewater purification, Prog. Org. Coat. 165 (2022) 106726, https://doi.org/10.1016/j.porgcoat.2022.106726.
[8] C. Yang, N. Han, C. Han, M. Wang, W. Zhang, W. Wang, Z. Zhang, W. Li, X. Zhang, Design of a Janus F-TiO2@PPS porous membrane with asymmetric wettability for switchable oil/water separation, ACS Appl. Mater. Interfaces 11 (2019) 22408–22418, https://doi.org/10.1021/acsami.9b05191.
[9] D. Li, J. Huang, G. Han, Z. Guo, A facile approach to achieve bioinspired PDMS@Fe3O4 fabric with switchable wettability for liquid transport and water collection, J. Mater. Chem. A 6 (2018) 22741–22748, https://doi.org/10.1039/C8TA08993K.
[10] Y. Li, L. He, X. Zhang, N. Zhang, D. Tian, External-field-induced gradient wetting for controllable liquid transport: from movement on the surface to penetration into the surface, Adv. Mater. 29 (2017) 1703802, https://doi.org/10.1002/adma.201703802.
[11] X. Hong, X. Gao, L. Jiang, Application of superhydrophobic surface with high adhesive force in No lost transport of superparamagnetic microdroplet, J. Am. Chem. Soc. 129 (2007) 1478–1479, https://doi.org/10.1021/ja065537c.
[12] X. Su, K. Li, H. Xie, Z. Chen, X. Li, W. Wu, Controllable hydrophilic/superhydrophobic patterned coatings for optical information encryption/decryption based on water-triggered opaque to translucent transition, J. Colloid Interface Sci. 654 (2024) 764–773, https://doi.org/10.1016/j.jcis.2023.10.093.
[13] F. Baig, Z. Zaheer, Z. Khan, F. Qasim, A comparative study of optical, reversible wettability and UV light sensitivity of ZnO nano-structures via chemical methods, Opt. Quantum Electron. 56 (2024) 715, https://doi.org/10.1007/s11082-024-06451-2.
[14] Y. Pan, W. Kong, B. Bhushan, X. Zhao, Rapid, ultraviolet-induced, reversibly switchable wettability of superhydrophobic/superhydrophilic surfaces, Beilstein J. Nanotechnol. 10 (2019) 866–873, https://doi.org/10.3762/bjnano.10.87.
[15] V.S. Yalishev, M. Iqbal, V.V. Kim, S.A. Khan, R.A. Ganeev, A.S. Alnaser, Reversible wettability transition of laser-textured metals after vacuum storing and low-temperature annealing, Appl. Phys. A 127 (2021) 393, https://doi.org/10.1007/s00339-021-04547-0.
[16] H.-Y. Ryu, S.H. Yoon, D.-H. Han, H. Hafeez, N.R. Paluvai, C.S. Lee, J.-G. Park, Fabrication of hydrophobic/hydrophilic switchable aluminum surface using poly(N-isopropylacrylamide), Prog. Org. Coat. 99 (2016) 295–301, https://doi.org/10.1016/j.porgcoat.2016.06.008.
[17] D. Li, L. Sun, L. Shi, L. Zhuo, L. Yang, J. Zhang, Y. Han, T. Ye, S. Wang, Reversible switchable wettability of intrinsic micro/nanostructured pollen microcarriers via pH-induce from superhydrophobicity to superhydrophilicity, Chem. Eng. J. 473 (2023) 145184, https://doi.org/10.1016/j.cej.2023.145184.
[18] H.-R. Zhang, W.-X. Ma, X.-Y. Han, G.-E. Chen, Z.-L. Xu, Intelligent pH-responsive PMIA membrane with reversible wettability for controllable oil/water and emulsion separation, Appl. Surf. Sci. 615 (2023) 156392, https://doi.org/10.1016/j.apsusc.2023.156392.
[19] S. Zhu, K. Tang, M. Liu, C. Sun, B. Bai, Ion-induced oil–water wettability alteration of rock surfaces. Part III: ion-bridging interactions between oil and solid, Chem. Eng. Sci. 252 (2022) 117275, https://doi.org/10.1016/j.ces.2021.117275.
[20] A. Quinn, R. Sedev, J. Ralston, Influence of the electrical double layer in electrowetting, J. Phys. Chem. B 107 (2003) 1163–1169, https://doi.org/10.1021/jp0216326.
[21] K. Wang, A. Naderi Bakhtiyari, Y. Wu, M. Liu, H. Zheng, Magneto-responsive wettability-switchable surfaces for in-situ large distance droplets capturing-releasing-bouncing, Chem. Eng. J. 478 (2023) 147420, https://doi.org/10.1016/j.cej.2023.147420.
[22] L. Wang, G. Wang, Y. Di, H. Wang, P. Wang, L. Dong, Y. Huang, G. Jin, Fast reversion of hydrophility-superhydrophobicity on textured metal surface by electron beam irradiation, Appl. Surf. Sci. 669 (2024) 160455, https://doi.org/10.1016/j.apsusc.2024.160455.
[23] W. Jiang, G. Wang, Y. He, X. Wang, Y. An, Y. Song, L. Jiang, Photo-switched wettability on an electrostatic self-assembly azobenzene monolayer, Chem. Comm. (2005) 3550–3552, https://doi.org/10.1039/B504479K.
[24] A. Uyama, S. Yamazoe, S. Shigematsu, M. Morimoto, S. Yokojima, H. Mayama, Y. Kojima, S. Nakamura, K. Uchida, Reversible photocontrol of surface wettability between hydrophilic and superhydrophobic surfaces on an asymmetric

diarylethene solid surface, Langmuir 27 (2011) 6395–6400, https://doi.org/10.1021/la2006524.
[25] X. Li, Y. Jiang, Z. Jiang, Y. Li, C. Wen, J. Lian, Reversible wettability transition between superhydrophilicity and superhydrophobicity through alternate heating-reheating cycle on laser-ablated brass surface, Appl. Surf. Sci. 492 (2019) 349–361, https://doi.org/10.1016/j.apsusc.2019.06.145.
[26] D. Li, M. Xiong, S. Wang, X. Chen, S. Wang, Q. Zeng, Effects of low-temperature plasma treatment on wettability of glass surface: molecular dynamic simulation and experimental study, Appl. Surf. Sci. 503 (2020) 144257, https://doi.org/10.1016/j.apsusc.2019.144257.
[27] T.F. O'Mahony, M.A. Morris, Hydroxylation methods for mesoporous silica and their impact on surface functionalisation, Microporous Mesoporous Mater. 317 (2021) 110989, https://doi.org/10.1016/j.micromeso.2021.110989.
[28] R.G. Acres, A.V. Ellis, J. Alvino, C.E. Lenahan, D.A. Khodakov, G.F. Metha, G. G. Andersson, Molecular structure of 3-aminopropyltriethoxysilane layers formed on silanol-terminated silicon surfaces, J. Phys. Chem. C 116 (2012) 6289–6297, https://doi.org/10.1021/jp212056s.
[29] S.G. Thakurta, A. Subramanian, Effect of hydrofluoric acid in oxidizing acid mixtures on the hydroxylation of silicon surface, J. Electrochem. Soc. 158 (2011) S19, https://doi.org/10.1149/1.3592760.
[30] B. Morel, L. Autissier, D. Autissier, D. Lemordant, B. Yrieix, D. Quenard, Pyrogenic silica ageing under humid atmosphere, Powder Technol. 190 (2009) 225–229, https://doi.org/10.1016/j.powtec.2008.04.049.
[31] A. D'Souza, C. Pantano, Hydroxylation and dehydroxylation behavior of silica glass fracture surfaces, J. Am. Ceram. Soc. 85 (2002) 1499–1504, https://doi.org/10.1111/j.1151-2916.2002.tb00303.x.
[32] W. Wang, M.W. Vaughn, Morphology and amine accessibility of (3-Aminopropyl) triethoxysilane films on glass surfaces, Scanning 30 (2008) 65–77, https://doi.org/10.1002/sca.20097.
[33] R.M. Pasternack, S. Rivillon Amy, Y.J. Chabal, Attachment of 3-(Aminopropyl) triethoxysilane on silicon oxide surfaces: dependence on solution temperature, Langmuir 24 (2008) 12963–12971, https://doi.org/10.1021/la8024827.
[34] M. Sypabekova, A. Hagemann, D. Rho, S. Kim, Review: 3-aminopropyltriethoxy-silane (APTES) deposition methods on oxide surfaces in solution and vapor phases for biosensing applications, Biosensors 13 (1) (2023) 36.
[35] C.F. Kwiatkowski, E. Andrews, D. Birnbaum, J. Bruton, J. DeWitt, C. Knappe, M. Maffini, A. Miller, J. Pelch, L. Reade, A. Soehl, R. Trier, X. Wang, T.F. Webster, Scientific basis for managing PFAS as a chemical class, Environ. Sci. Processes Impacts 7 (2020) 532–543, https://doi.org/10.1021/acs.estlett.0c00255.
[36] L. Van Daele, B. Van de Voorde, R. Colenbier, L. De Vos, L. Parmentier, L. Van der Meeren, A. Skirtach, R.I. Dmitriev, P. Dubruel, S. Van Vlierberghe, Effect of molar mass and alkyl chain length on the surface properties and biocompatibility of poly (alkylene terephthalate)s for potential cardiovascular applications, J. Mater. Chem. B 11 (2023) 10158–10173, https://doi.org/10.1039/D3TB01889J.
[37] W. Chen, V. Karde, T.N.H. Cheng, S.S. Ramli, J.Y.Y. Heng, Surface hydrophobicity: effect of alkyl chain length and network homogeneity, Front. Chem. Sci. Eng. 15 (2021) 90–98, https://doi.org/10.1007/s11705-020-2003-0.
[38] C.F. Kwiatkowski, E. Andrews, D. Birnbaum, J. Bruton, J. DeWitt, C. Knappe, M. Maffini, A. Miller, J. Pelch, L. Reade, A. Soehl, R. Trier, X. Wang, T.F. Webster, Scientific basis for managing PFAS as a chemical class, Environ. Sci. Processes Impacts 7 (2020) 532–543, https://doi.org/10.1021/acs.estlett.0c00255.
[39] Y. Wang, Y. Sun, Y. Xue, X. Sui, B. Yuan, Y. Wang, W. Liang, Functional surfaces with reversibly switchable wettability: fundamentals, progresses, applications and challenges, Prog. Org. Coat. 188 (2024) 108167, https://doi.org/10.1016/j.porgcoat.2023.108167.
[40] A. Roy, H. Ullah, M. Alzahrani, A. Ghosh, T.K. Mallick, A.A. Tahir, Synergistic effect of Paraffin-Incorporated In2O3/ZnO Multifold smart glazing composite for the self-cleaning and energy-saving built environment, ACS Sustain. Chem. Eng. 10 (2022) 6609–6621, https://doi.org/10.1021/acssuschemeng.2c00260.
[41] W. Zhao, Y. Zhan, W. Li, S. Hao, A. Amirfazli, Application of 3D printing for fabrication of superhydrophobic surfaces with reversible wettability, RSC Adv. 14 (2024) 17684–17695, https://doi.org/10.1039/D4RA02742F.